

Characterization of Turbulence and Deterministic Stresses through Phase-Dependent Measurements in the Near Wake of a Wind Turbine in an Infinite Turbine Array

N.M. Hamilton¹, M. Tutkun² and R.B. Cal¹

¹Department of Mechanical and Materials Engineering
Portland State University, Portland, Oregon, 97201, USA

²Institute for Energy Technology, Kjeller, Norway

Abstract

A wind tunnel experiment was conducted to investigate the evolution of the stress field in the wake of a wind turbine in the fully developed turbine canopy layer. Phase-locked stereo particle image velocimetry measurements were taken in planes parallel to the turbine rotor and progressing throughout the near wake. Stresses vary significantly as a function of phase angle of the turbine rotor blades. The resupply of kinetic energy to the momentum-deficit area of the wake is accomplished largely through the flux term in the mean kinetic energy equation. Phase-dependent contributions to the total flux into the wake indicate that turbulent structures impart periodic increases in entrainment of high-momentum fluid. Deviations of phase-averaged velocities from total mean values are used to formulate deterministic stresses, which make smaller overall contributions to the flux of kinetic energy into the wake.

Introduction

The turbulent wakes of wind turbines has been discussed in some detail for individual devices (e.g. [11, 13]) but only recently has the interaction between wakes in large arrays been investigated. Complex flow generated by atmospheric forcing and interaction with rotating blades is still the subject of interest in making wind energy more productive and efficient to help meet the increasing energy demands worldwide.

Numerical simulations [3, 12] have been a common means of researching full wakes and wake interaction in infinite wind turbine arrays. The idea of the ‘infinite’ array of wind turbines arose from the observation that a periodicity of turbulence statistics exists in regularly arranged wind farms beyond the fourth row of devices [3, 4]. The periodicity in the stream-wise spatial coordinate allows the convective and pressure gradient terms to be effectively omitted from the energy balance for wind turbines.

Phase-related flow effects have been investigated for wind turbines by Lignarolo [9] and Hu [7] illuminating the development of tip vortices evolving from the blades under various operating conditions. The significance of phase or standing waves in turbulent flows was formulated through a triple decomposition [10] of velocity measurements. Deterministic stresses have been shown to be significant in turbomachinery by Adamczyk [1].

The current work undertakes to decompose velocity measurements in planes spanning a wind turbine wake into phase-averaged and deterministic components. The flux of kinetic energy, responsible for much of the resupply of high-momentum flow into the wake [2, 6, 5], it formulated with the phase-averaged and deterministic stresses.

Theory

The mean kinetic energy equation in a wind turbine boundary

layer can be described through a slightly modified set of turbulent boundary layer equations.

$$U_j \frac{\partial \frac{1}{2} U_i^2}{\partial x_j} = -\frac{U_i}{\rho} \frac{\partial P}{\partial x_i} + \overline{u_i u_j} \frac{\partial U_i}{\partial x_j} - \frac{\partial \overline{u_i u_j} U_i}{\partial x_j} - \mathcal{F}_{x_i} \quad (1)$$

Above, the forcing term \mathcal{F}_{x_i} represents the thrust force added to the flow as power is extracted by the wind turbine device. In many studies of wind turbine wakes [2, 6, 5, 8] the unsteady term is omitted from the mean kinetic energy budget through ensemble averaging of a large set of random samples in the period flow of wake. With the infinite array assumption equation (1) reduces to a balance between the flux of kinetic energy, the production of turbulence, and the thrust force from the wind turbine.

The Reynolds stress tensor is significant to the overall momentum balance in the wind turbine boundary layer. It contributes directly to the flux of kinetic energy and production of turbulence terms (third and fourth terms in the right hand side of equation (1)) and can account for a relatively large portion of the total kinetic energy in the turbine canopy.

The conventional description of the Reynolds stress tensor positions normal stresses along the diagonal of the tensor and symmetrically distributes the shear terms in off-diagonal positions. In polar-cylindrical coordinates the turbulent stress tensor is written,

$$\begin{aligned} \overline{u_i u_j} &= \overline{(\tilde{u}_i - U_i)(\tilde{u}_j - U_j)} \\ &= \begin{bmatrix} \overline{u_x u_x} & -\overline{u_x u_r} & -\overline{u_x u_\theta} \\ -\overline{u_r u_x} & \overline{u_r u_r} & -\overline{u_r u_\theta} \\ -\overline{u_\theta u_x} & -\overline{u_\theta u_r} & \overline{u_\theta u_\theta} \end{bmatrix} \end{aligned} \quad (2)$$

where the x , r , and θ subscripts refer to the axial, radial, and azimuthal coordinates, respectfully. In the following discussion and figures, the phase angle and azimuthal coordinate are distinguished as ϕ and θ , respectively.

The total Reynolds stress denoted in equation (2) is ensemble averaged over all measurements, regardless of phase angle of the turbine rotor. Throughout the following, a capital letter or an overbar indicates that a quantity has been averaged over time, rendering the quantity independent of phase. Angle brackets indicate that phase-dependent quantities have been averaged. Making an average of phase-dependent values over all phase angles yields an approximation of the time-averaged quantity.

Measurements made at particular phase angles of the rotor blades yield a set of phase-averaged deviations from time averaged quantities. These deviations can be multiplied and ensemble averaged to acquire deterministic stresses [1, 10].

$$\overline{u_i'' u_j''} = \overline{(U_i - \langle u_i \rangle)(U_j - \langle u_j \rangle)} \quad (3)$$

The total flux of kinetic energy can be then decomposed into turbulent, phase-dependent, and deterministic contributions. Considering the velocities in a cylindrical coordinate system, the

component of the flux tensor bring high-momentum flow into the wake can be written as,

$$F_{xr} = \overline{u_x u_r} U_x = \left(\overline{\langle u_x u_r \rangle_\phi} + \overline{u_x'' u_r''} \right) U_x \quad (4)$$

Experiment

Measurements of a wind turbine wake in the fully developed canopy layer were made in the wind tunnel at Portland State University. The wind tunnel was furnished with a passive grid at the entrance of the test section to introduce turbulence, removable vertical strakes shaped to precondition the boundary layer to in the wind tunnel to more closely match observed the atmospheric boundary layer, and semi-porous surface roughness via small-diameter chains. Characteristic profiles of the approach flow to the model array are presented in *Statistical development of wind turbine wakes for the fully developed wind turbine array boundary layer characterized via wall-normal-spanwise planes* by Hamilton and Cal.

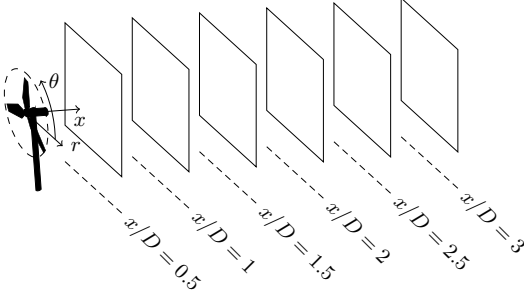


Figure 1: Schematic of a model wind turbine with and measurement planes across the wake. Flow is from left to right. The turbine shown is in the fully developed region of the wind turbine array.

Figure 1 shows an example turbine from the current experiment. In the figure measurement locations accessed through $2D - 3C$ stereographic particle image velocimetry (SPIV) are shown as well as the polar-cylindrical coordinate system used in the following analysis. Measurements were made behind a wind turbine in the fully developed region, the fourth row for arrays arranged in a Cartesian grid. Rows of turbines were spaced six rotor diameters apart (72 cm) and columns separated by 3 rotor diameters (36 cm) hub to hub.

The wind turbine models were fabricated in-house and consist of a hollow steel mast and rotor blades cut from 0.5 mm sheet steel. The blades of the turbine were given pitch and twist via a press to ensure uniformity. Each blade was pitched approximately $\gamma_{root} = 22^\circ$ out of the rotor plane at the root of the blade and had a 7° twist from root to tip, resulting in a pitch of $\gamma_{tip} 15^\circ$ at the tip of each blade. The nacelle of each turbine was composed of a DC electric motor, loaded with resistive elements to slow the rotation of the turbine blades, allowing each row of turbines to be matched to its peak power coefficient. Model wind turbines were mounted in steel plates (0.75 cm thick) spanning the wind tunnel. Figure 2 shows details of the model wind turbines.

The position of the rotor blade was located with a Monarch remote optical sensor placed outside the wind tunnel and able to see a small square of reflective tape affixed to one blade of the rotor. With each pass of the tape the sensor initiated a square wave signal that in turn triggered the SPIV measurements. Four positions of the rotor were considered in the experiment, $\phi \in [0^\circ, 30^\circ, 60^\circ, 90^\circ]$, where 0° was one blade oriented

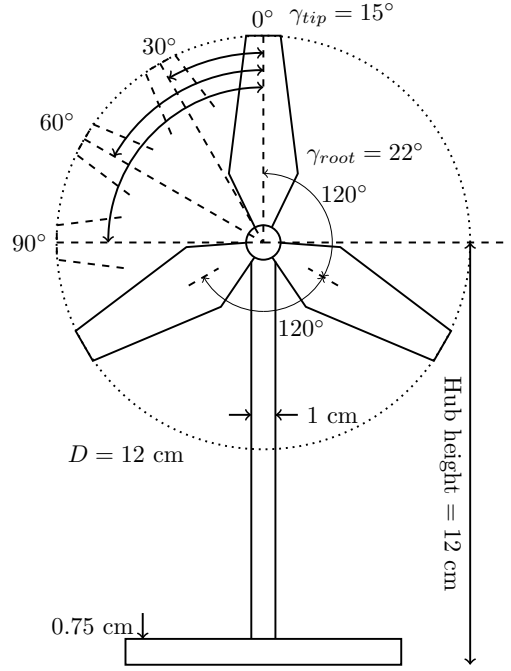


Figure 2: Schematic of a fully assembled wind turbine model including the mast and a section of the mounting plate. The phase angles indicated are measured from the position of a single blade at top-dead-center.

vertically upward, rotating clockwise facing the front of the turbine.

Results

The momentum deficit of the wake of the wind turbine is visible in the contours of the mean axial (streamwise) velocity U_x shown in figure 3. The minimum value of $U_x = 0.5 \text{ ms}^{-1}$ occurs directly following the nacelle of the model wind turbine at $x/D = 0.5$. In the conditions of this experiment it is not uncommon to see recirculation in this location in an instantaneous sense especially in leading row wind turbines. However, over a large set of samples any negative axial velocities are washed out.

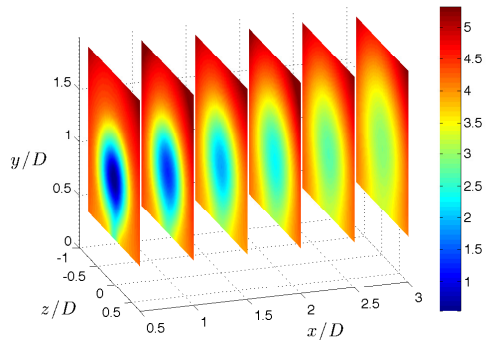


Figure 3: Time averaged streamwise velocity, U_x . The contours above show the mean velocity averaged over all measurements and are independent of phase.

The choice of polar-cylindrical coordinate system is intuitive given the geometry and operation of the wind turbines. When viewed in this sense, the dominant Reynolds stresses contributing to the energy budget are the normal stress $\overline{u_x^2}$ and the shear stress $-\overline{u_x u_r}$ (figures 4 and 5, respectively). The second order quantities show the growth of the wake more clearly than the mean velocities.

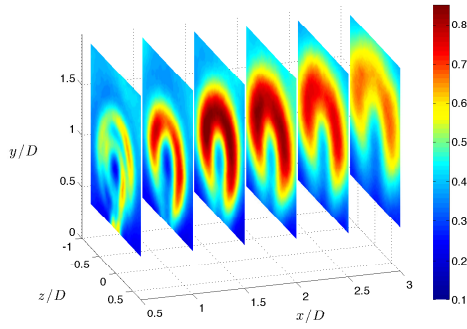


Figure 4: Time averaged Reynolds normal stress composed of fluctuations of axial velocity, $\overline{u_x^2}$. The contours above show the mean velocity averaged over all measurements and are independent of phase.

Peak values of $\overline{u_x^2}$ occur approximately $x/D = 1.5$ downstream from the wind turbine rotor similar to previous studies of wind turbine wakes [5, 6]. The axial normal stress is on the order of $1 \text{ m}^2\text{s}^{-2}$, more than twice the magnitude of the radial and azimuthal normal stresses (not shown for brevity). Contributions to the overall flux of kinetic energy by $\overline{u_x^2}$ are small due to gradients that are small in the streamwise direction compared to those along the radial coordinate.

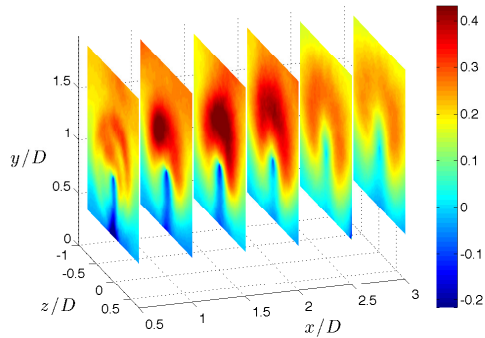


Figure 5: Time averaged Reynolds shear stress composed of axial and radial fluctuations of velocity, $-\overline{u_x u_r}$. The contours above show the mean velocity averaged over all measurements and are independent of phase.

In many wind energy studies (e.g. [2, 6]) the Reynolds shear stress composed of the streamwise and wall-normal fluctuations is discussed as its contribution to the flux and production terms of the kinetic energy budget is the most significant. The analog to this term in the polar-cylindrical coordinate system is $-\overline{u_x u_r}$ which describes turbulence involving streamwise variations and those radially inward or outward from the hub. Figure 5 shows that the $-\overline{u_x u_r}$ is positive for most of the near wake, with the exception being directly behind the mast of the wind turbine. The contours of $-\langle u_x u_r \rangle_{30^\circ} U_x$ and $-\langle u_x u_r \rangle_{60^\circ} U_x$ show regions in the near wake where the flux is of greater magnitude than the average because the position of the rotor allows the flow to be advected into the wake. For other phase angles, the blades disturb the direct advection into the wake.

The above statistics have been shown in a time-averaged sense. The flux of kinetic energy has been formulated in figure 6 in a phase-averaged sense to demonstrate that there are periodic contributions to the entrainment of kinetic energy. Typically this quantity is discussed as bringing high-momentum flow into the wake from above the turbine canopy. In the current formulation $-\langle u_x u_r \rangle_\phi U_x$ shows the flux radially inward or outward. The general trend of the flux of kinetic energy is into the wake from outside. Below the nacelle of the wind turbine there are a few areas in which the flux of kinetic energy is away from the center of the wake as seen in $-\langle u_x u_r \rangle_{30^\circ} U_x$ and $-\langle u_x u_r \rangle_{60^\circ} U_x$.

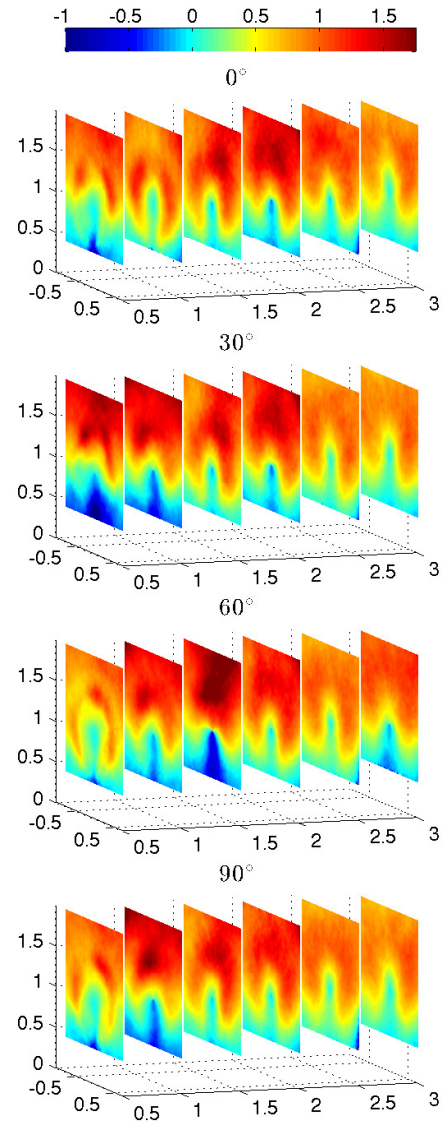


Figure 6: Phase-averaged contours of the flux of kinetic energy $\langle u_x u_r \rangle_\phi U_x$.

A further consideration for the flux of kinetic energy is the contribution by the deterministic stresses from equation 3, shown in figure 7. Although the turbulent stresses show significant dependence on the orientation of the rotors, the deterministic stresses are approximately two orders of magnitude smaller. The deterministic shear stress $-\overline{u_x'' u_r''}$ demonstrates periodic values in the azimuthal coordinate θ around the rotor diameter. The contours in figure 7 represent the wave-like contribution added to the mean flow field. They are independent of orientation of the rotor blades and can be viewed as the underlying periodicity in the wake.

The flux composed of the deterministic stresses is shown in figure 8. The magnitude of this contribution, like the stresses above, is approximately two orders of magnitude smaller than the phase-dependent or time averaged quantities. The magnitudes of the flux composed with the deterministic stresses indicates that the periodic contributions to the total behavior can be neglected at the first order.

Conclusions

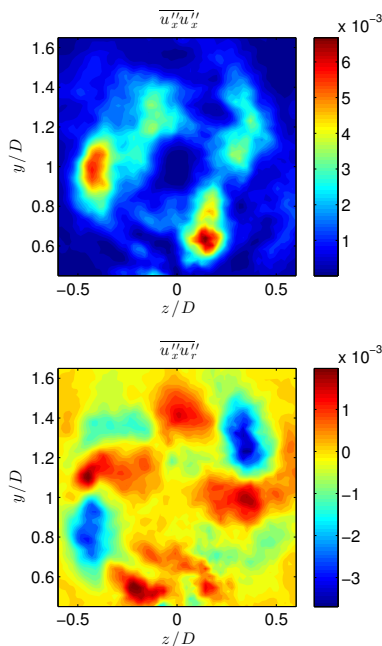


Figure 7: Normal (top) and shear (bottom) deterministic stresses composed of ensemble averaged deviations between phases

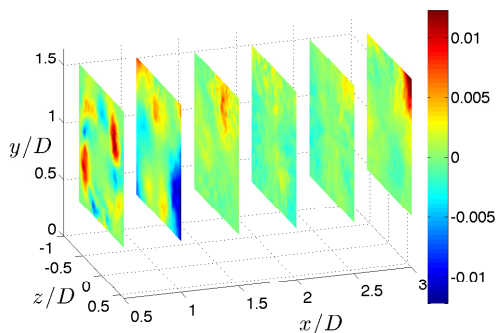


Figure 8: Contours representing the contribution of the total flux by the deterministic stress $-u_x''u_z''$.

The current experiment made phase-locked $2D-3C$ stereo PIV measurements across the wake of a wind turbine in a fully-developed wind farm. The total mean values of axial velocity show the momentum deficit area in the near wake quite clearly but it is in the turbulent stresses that the growth of the wake is most easily distinguished.

The flux of kinetic energy is composed with the phase-averaged shear stress and compared showing that entrainment of high momentum flow is predominantly into the center of the wake radially. Following the rotor blades in certain orientations, there is flux of kinetic energy out of the wake below hub height.

Deterministic stresses representing the combined deviations of phase-averaged velocities from the total mean quantities are approximately two orders of magnitude smaller than turbulent stresses. This difference in magnitude arises from the nature of the flow forcing the passage of the rotors, as opposed to other turbomachinery where the flow is forced by the blades. Although the deterministic contribution to the flux of kinetic energy is smaller in magnitude, there is some theoretical interest arising from azimuthal periodicity at the rotor diameter. That the deterministic stresses make a small contribution to the overall behavior suggests that they may merit further investigation. Alternate decompositions directly quantifying deviations of phase-locked stresses from time-averaged values may be of more interest in terms of the flux of kinetic energy.

An experiment detailing the evolution of turbulence statistics throughout the near and far wake for an identical experimental arrangement can be found in *Statistical development of wind turbine wakes for the fully developed wind turbine array boundary layer characterized via wall-normal-spanwise planes* by Hamilton, Tutkun, and Cal, presented in the current conference.

References

- [1] Adamczyk, J. J., Aerodynamic analysis of multistage turbomachinery flows in support of aerodynamic design, *Journal of Turbomachinery*, **122**, 2000, 189–217.
- [2] Cal, R. B., Lebrón, J., Castillo, L., Kang, H. S. and Meneveau, C., Experimental study of the horizontally averaged flow structure in a model wind-turbine array boundary layer, *Journal of Renewable and Sustainable Energy*, **2**, 2010, 013106.
- [3] Calaf, M., Meneveau, C. and Meyers, J., Large eddy simulation study of fully developed wind-turbine array boundary layers, *Physics of Fluids*, **22**, 2010, 015110.
- [4] Chamorro, L. P., Arndt, R. and Sotiropoulos, F., Reynolds number dependence of turbulence statistics in the wake of wind turbines, *Wind Energy*, **15**, 2012, 733–742.
- [5] Hamilton, N., Cal, R. B. and Melius, M., Wind turbine boundary layer arrays for cartesian and staggered configurations: *Part I*, flow field and power measurements, *Wind Energy*, 2014, DOI:http://dx.doi.org/10.1002/we.1697.
- [6] Hamilton, N., Kang, H. S., Meneveau, C. and Cal, R. B., Statistical analysis of kinetic energy entrainment in a model wind turbine array boundary layer, *Journal of Renewable and Sustainable Energy*, **4**, 2012, 063105.
- [7] Hu, H., Yang, Z. and Sarkar, P., Dynamic wind loads and wake characteristics of a wind turbine model in an atmospheric boundary layer wind, *Experiments in fluids*, **52**, 2012, 1277–1294.
- [8] Lebrón, J., Castillo, L. and Meneveau, C., Experimental study of the kinetic energy budget in a wind turbine streamtube, *Journal of Turbulence*, **13**.
- [9] Lignarolo, L., Ragni, D., Krishnaswami, C., Chen, Q., Simão Ferreira, C. and Van Bussel, G., Experimental analysis of the wake of a horizontal-axis wind-turbine model, *Renewable Energy*.
- [10] Reynolds, W. and Hussain, A., The mechanics of an organized wave in turbulent shear flow. part 3. theoretical models and comparisons with experiments, *Journal of Fluid Mechanics*, **54**, 1972, 263–288.
- [11] Snel, H., Review of aerodynamics for wind turbines, *Wind Energy*, **6**, 2003, 203–211.
- [12] Troldborg, N., Larsen, G. C., Madsen, H. A., Hansen, K. S., Sørensen, J. N. and Mikkelsen, R., Numerical simulations of wake interaction between two wind turbines at various inflow conditions, *Wind Energy*, **14**, 2011, 859–876.
- [13] Vermeer, L. J., Sørensen, J. N. and Crespo, A., Wind turbine wake aerodynamics, *Progress in aerospace sciences*, **39**, 2003, 467–510.